OPEN

Aluminum enhances inflammation and decreases mucosal healing in experimental colitis in mice

G Pineton de Chambrun[1,2,3,4,12], M Body-Malapel[1,2,3,12], I Frey-Wagner[5], M Djouina[1,2,3], F Deknuydt[6,7,8], K Atrott[5], N Esquerre[1,2,3], F Altare[6,7,8], C Neut[1,2,3,9], MC Arrieta[10], T-D Kanneganti[11], G Rogler[5], J-F Colombel[1,2,3,4], A Cortot[1,2,3,4], P Desreumaux[1,2,3,4] and C Vignal[1,2,3]

The increasing incidence of inflammatory bowel diseases (IBDs) in developing countries has highlighted the critical role of environmental pollutants as causative factors in their pathophysiology. Despite its ubiquity and immune toxicity, the impact of aluminum in the gut is not known. This study aimed to evaluate the effects of environmentally relevant intoxication with aluminum in murine models of colitis and to explore the underlying mechanisms. Oral administration of aluminum worsened intestinal inflammation in mice with 2,4,6-trinitrobenzene sulfonic acid- and dextran sodium sulfate-induced colitis and chronic colitis in interleukin 10-negative (IL10$^{-/-}$) mice. Aluminum increased the intensity and duration of macroscopic and histologic inflammation, colonic myeloperoxidase activity, inflammatory cytokines expression, and decreased the epithelial cell renewal compared with control animals. Under basal conditions, aluminum impaired intestinal barrier function. *In vitro*, aluminum induced granuloma formation and synergized with lipopolysaccharide to stimulate inflammatory cytokines expression by epithelial cells. Deleterious effects of aluminum on intestinal inflammation and mucosal repair strongly suggest that aluminum might be an environmental IBD risk factor.

INTRODUCTION

Inflammatory bowel diseases (IBDs), which include Crohn's disease and ulcerative colitis, are chronic diseases characterized by an excessive uncontrolled intestinal inflammation resulting from an abnormal immune response to commensal microbiota in a susceptible host.[1] In the past 10 years, genetic research in IBD has been particularly fruitful. However, among the many susceptibility genes identified (>100 to date) none were demonstrated to be necessary or sufficient for disease onset.[2,3] The spatial heterogeneity of Crohn's disease and ulcerative colitis, their increasing incidence and prevalence with time and in different regions around the world, the low concordance rate in monozygotic twins and the increased risk among migrants from low-incidence to high-incidence areas are strong arguments implying an important role for environmental factors in the pathogenesis of IBD.[4,5] However, besides smoking and appendectomy and, more recently, exposure to antibiotics in childhood, no strong environmental factors have been identified to date.[6–9]

The increase of IBD in developing countries has focused attention on the potential role of industrialization and environmental pollutants as causative environmental factors in their pathophysiology.[10,11] Twentieth century industrialization has led to an increased accumulation of heavy metals, and in particular aluminum, in our surrounding ecosystems. Aluminum is ubiquitous and is the most abundant metal element in our environment.[12,13] In the past 50 years, worldwide production of aluminum has regularly increased, from <5 million tons in 1960 to >25 million tons in 2002, and developed countries have raised their current domestic consumption by 350%.[14,15] A main route of exposure to aluminum for the general population is through food and water. The decline in the use of unprocessed foods and the increased consumption of cakes, pastries, and sugar-rich foods characterizing 'food

[1]Univ Lille Nord de France, Lille, France. [2]Inserm U995, Lille, France. [3]UDSL, Lille, France. [4]Hepato-Gastroenterology Department, CHU Lille, Lille, France. [5]Division of Gastroenterology and Hepatology, University Hospital Zurich, Zurich, Switzerland. [6]INSERM, UMR892, Nantes, France. [7]CNRS, UMR6299, Nantes, France. [8]Université de Nantes, Nantes, France. [9]Clinical Bacteriology, College of Pharmacy, Lille, France. [10]Finlay Lab, Michael Smith Laboratories, University of British Columbia, Vancouver, British Columbia, Canada and [11]Department of Immunology, St Jude Children's Research Hospital, Memphis, Tennessee, USA. Correspondence: C Vignal (cecile_vignal@hotmail.com)
[12]Shared first authorship.

Received 9 January 2013; revised 12 August 2013; accepted 14 August 2013; published online 16 October 2013. doi:10.1038/mi.2013.78

westernization' has resulted in an increased ingestion of aluminum, which exceeds the tolerable weekly intake of 7 mg kg^{-1} per week in a significant proportion of the European and North American populations.[16] For many years, exposure to aluminum was suggested to favor an abnormal immune response in different diseases, including autoimmune conditions.[17] However, despite this known toxicity and a potential gut interaction, aluminum and its effect on intestinal homeostasis and inflammation have not been investigated so far, particularly in the physiopathology of IBD.

The aim of our study was to explore the pro-inflammatory role of aluminum in different models of chemically induced and chronic colitis in mice. Particular attention was paid to the interaction between aluminum and epithelial cells and its role in the immune response against bacteria.

RESULTS

Aluminum worsens colitis induced by 2,4,6-trinitrobenzene sulfonic acid and dextran sodium sulfate in mice

In a first set of experiments, C57BL6 mice were fed for 4 weeks with aluminum citrate (AluCi) or aluminum phosphate (AluP) at a concentration of 1.5 mg Al element kg^{-1} per day. These four weeks' oral administration of aluminum did not induce any macroscopic, histological, or molecular colonic inflammation (**Supplementary Figure 1** online). In another set of experiments, C57BL6 mice were treated with AluCi or AluP for 4 weeks before rectal administration of 2,4,6-trinitrobenzene sulfonic acid (TNBS; **Figure 1a**). Four days after colitis induction, the severity of intestinal inflammation was assessed by macroscopic, histological, and molecular parameters. Macroscopic Wallace score of colonic inflammation was significantly increased in both forms of aluminum-treated mice compared with phosphate buffer saline (PBS)-treated mice (**Figure 1b**). Aluminum-treated mice presented more severe and extended macroscopic inflammation of the colon with large areas of ulceration (data not shown). Consistently, at the microscopic level, the histological Ameho score of colonic inflammation was more severe in both forms of aluminum-treated mice compared with PBS-treated mice, leading to more extensive ulceration and necrosis involving 80% of the whole colon (**Figure 1c,d**). Myeloperoxidase (MPO) activity reflecting neutrophil infiltration was also significantly higher in aluminum-treated mice compared with PBS-treated mice (**Figure 1e**).

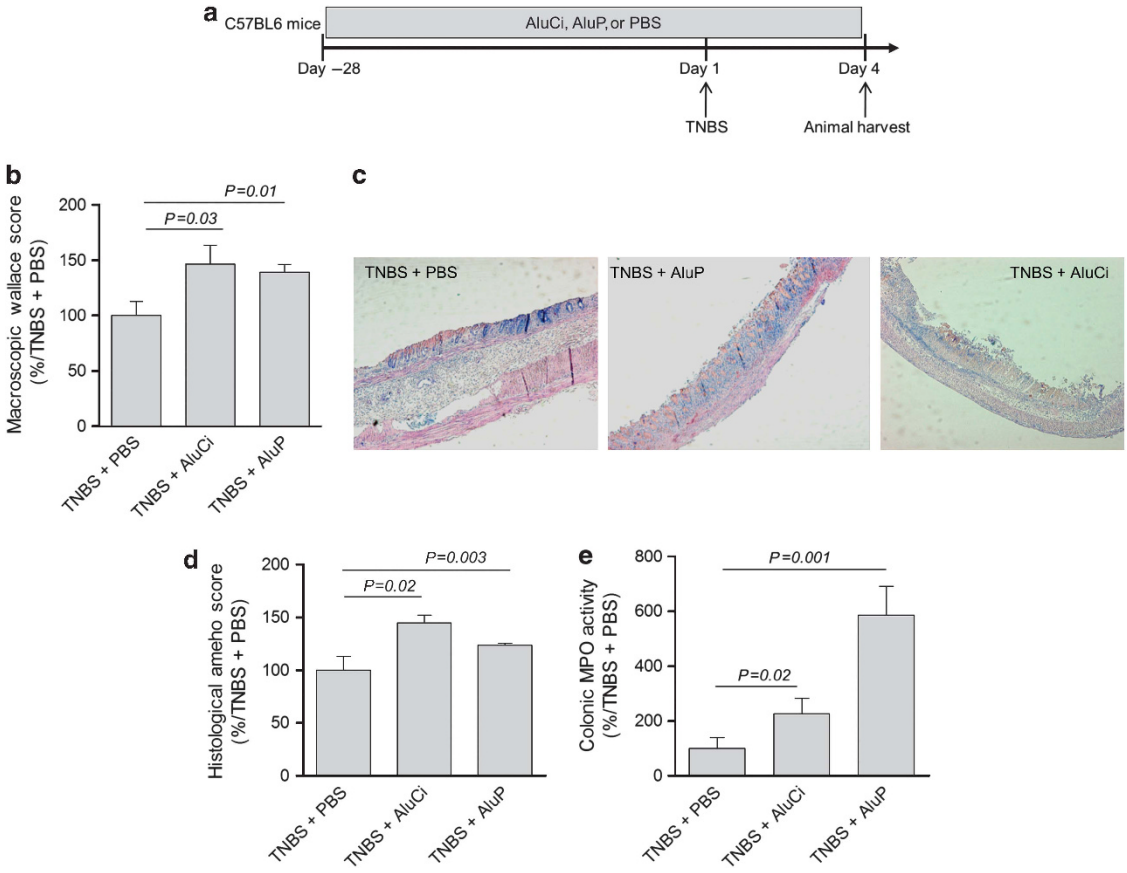

Figure 1 Aluminum worsens 2,4,6-trinitrobenzene sulfonic acid (TNBS)-induced colitis. (**a**) C57BL6 mice ($n = 14$ per group) were fed with aluminum citrate (AluCi) or aluminum phosphate (AluP) (1.5 mg of Al element kg^{-1} per day) or with phosphate buffer saline (PBS) for 31 days. At day 28, colitis was induced by intrarectal administration of TNBS. Four days after colitis induction, mice were euthanized and colitis parameters were assessed. (**b**) The macroscopic Wallace score was determined as described in Methods. (**c**, **d**) Histopathological changes in colon tissues were examined by May-Grünwald and Giemsa (MGG) staining and scoring was performed as described in Methods. (**e**) Myeloperoxidase (MPO) activity was measured in colonic lesions. Results are expressed as the percentage of variation compared with TNBS-treated mice.

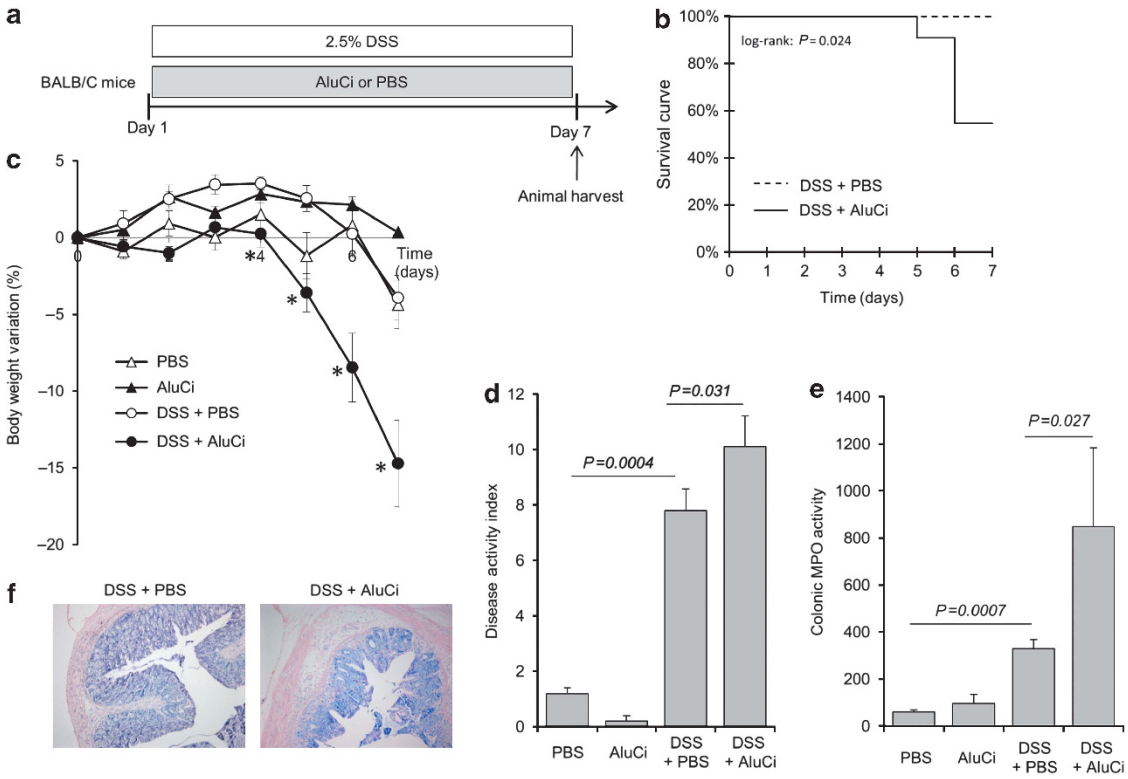

Figure 2 Aluminum citrate (AluCi) worsens dextran sodium sulfate (DSS)-induced colitis. (**a**) BALB/C mice ($n = 10$ per group) were treated with 2.5% DSS and AluCi (1.5 mg of Al element kg^{-1} per day) or phosphate buffer saline (PBS) for 7 days. Control mice treated with AluCi or PBS without DSS were followed for the same period ($n = 5$ per group). (**b**) Survival of mice was monitored until day 7 after the start of DSS. (**c**) Body weight was scored daily. * means $P < 0.05$ between DSS ± PBS and DSS ± AluCi. (**d**) A disease activity index that included body weight variation, the presence of blood in stools, and stool consistency was calculated at day 7. (**e**) Myeloperoxidase (MPO) activity was measured on colons harvested at day 7. (**f**) Histopathological changes of colonic tissues were examined by May-Grünwald and Giemsa (MGG) staining.

To complete our understanding of the detrimental effect of aluminum observed in TNBS-induced colitis, BALB/C mice were concomitantly treated by aluminum gavage and oral administration of dextran sodium sulfate (DSS) 2.5% in drinking water for 7 days (**Figures 2a** and **3a**). A 2-fold increased mortality was observed in AluCi-treated mice with DSS-induced colitis compared with control animals (**Figure 2b**). Moreover, mice treated with DSS and AluCi or AluP had more than a 3- and 2-fold body weight loss, respectively, compared with DSS and PBS-treated mice (**Figures 2c** and **3b**). The body weight loss occurred at the lowest aluminum concentration of 0.15 mg kg^{-1} per day and was more pronounced with higher doses such as 1.5 and 15 mg kg^{-1} per day (**Figure 3b**). The disease activity index (DAI), combining weight loss, stool consistency, and the presence of rectal bleeding, was also increased in both forms of aluminum-treated mice compared with PBS-treated mice with colitis (**Figures 2d** and **3c**). Consistently, colonic MPO activity was increased in aluminum-treated mice compared with control animals, with colitis together with a more intense inflammatory infiltrate mainly located in the mucosal and submucosal layers (**Figure 2e,f**). To demonstrate that our results were specific to aluminum, mice were fed with another metal, namely zinc phosphate (ZnP) together with colitis induction (**Figure 3a**). Mice treated with ZnP experienced the same body weight loss as DSS- and PBS-treated mice and no difference in DAI was observed (**Figure 3b,c**). As a whole, these results demonstrated that two different forms of aluminum worsened lesions severity in two distinct models of colitis in mice.

Aluminum worsens chronic colitis in interleukin 10-negative mice

We then investigated the effects of aluminum in a chronic colitis model. Interleukin 10-negative ($IL10^{-/-}$) mice received AluCi in their drinking water for 7 weeks with a daily dose of 1.5 mg Al element per kg body weight (**Figure 4a**). Macroscopic mucosal damage was assessed by mini-endoscopy score (**Figure 4b,c**). Mucosa from $IL10^{-/-}$ mice receiving water showed overt signs of inflammation. $IL10^{-/-}$ mice treated with AluCi had a mucosa less transparent, a vascular pattern more altered, more fibrin and a significant increase in mucosa granularity compared with $IL10^{-/-}$ mice receiving water. The histological score for $IL10^{-/-}$ mice treated with AluCi was significantly increased compared with the water-treated $IL10^{-/-}$ mice (**Figure 4d,e**). MPO activity was significantly more elevated in AluCi-treated $IL10^{-/-}$ mice than in control $IL10^{-/-}$ mice (**Figure 4f**). Taken together, these data argued in favor of a worsening effect of oral aluminum on the development of chronic colitis in $IL10^{-/-}$ mice.

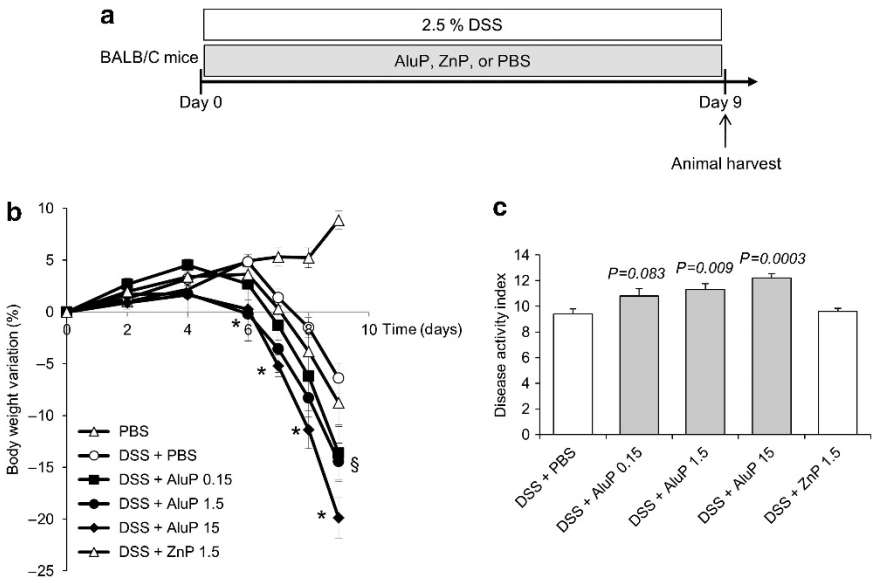

Figure 3 Aluminum phosphate (AluP) but not zinc phosphate (ZnP) worsens dextran sodium sulfate (DSS)-induced colitis. (**a**) BALB/C mice ($n = 10$ per group) were treated with 2.5% DSS and with increasing doses of AluP (0.15, 1.5, and 15 mg of Al element kg^{-1} per day) or ZnP (1.5 mg of Zn element kg^{-1} per day) or phosphate buffer saline (PBS) for 9 days. (**b**) Body weight was scored daily. * means $P < 0.05$ between DSS ± PBS and DSS ± AluP 1.5 and 15, § means $P < 0.05$ between DSS ± PBS and DSS ± AluP 0.15. (**c**) A disease activity index that included body weight variation, the presence of blood in stools, and stool consistency was calculated at day 9.

Aluminum increases the inflammatory cytokine expression in different models of colitis

AluCi significantly increased the expression of *Il1β* and *Il17a* mRNA in the colon of animals 4 days after TNBS administration (**Figure 5a**). The modification of this colonic cytokine profile induced by aluminum gavage and TNBS administration was associated with an increased expression of *Nlrp3* mRNA (**Figure 5a**), a known intracellular innate immune marker of inflammasome response regulated by aluminum.[18] Similar data were obtained in animals with DSS-induced colitis, where AluCi administration also significantly upregulated the colonic expression of inflammatory cytokines and *Nlrp3* mRNA compared with untreated mice with colitis (**Figure 5b**). Similar results were observed with AluP (data not shown).

In the chronic model of colitis, mucosal levels of *Il1β*, *Il17α*, and *Nlrp3* tended to be higher in the $IL10^{-/-}$ mice intoxicated with AluCi compared with $IL10^{-/-}$ mice receiving water (**Figure 5c**).

Enhanced inflammatory cytokine expression in aluminum-treated epithelial cells and potentiation by bacterial components

To investigate the potential inflammatory effect of luminal aluminum on the first intestinal layer in contact with luminal antigens and particles, we incubated HT-29 and Caco-2 epithelial cells for 3 h with increased concentrations of aluminum from 10 to 100 μg of Al element/ml^{-1}. A dose-response effect of aluminum was observed in Caco-2 cells, leading to an increased expression of the inflammatory cytokines IL8 and IL1β mRNA (**Figure 6a**). Similar data were obtained with HT-29 epithelial cells (data not shown). Co-incubation of Caco-2 cells with a low concentration of bacterial lipopolysaccharide (LPS, 1 μg ml^{-1}) and increased concentrations of aluminum led to a synergistic and dose-dependent pro-inflammatory effect with an increased expression of IL8 and IL1β mRNA (**Figure 6b**). Similar data were obtained in HT-29 cells (data not shown).

Aluminum extends colitis duration and decreases the mucosal healing

Besides its effects on colitis severity, we investigated the influence of oral administration of AluCi at 1.5 mg Al element kg^{-1} on colitis duration in C57BL6 mice submitted to one cycle of 2% DSS for 7 days (**Figure 7a**). Colonic lesions were evaluated during the 19-days experiment to investigate the persistence of lesions during the recovery period. At the end of DSS administration, mice treated with aluminum continued to lose weight and presented a slow recovery compared to mice with colitis receiving the vehicle (**Figure 7b**). In contrast, body weight changes were paralleled after day 7 in control mice with or without DSS-induced colitis receiving the vehicle and control animals treated with aluminum (**Figure 7b**). At day 19, animals with DSS-induced colitis receiving aluminum presented persistent intestinal inflammation, as demonstrated by an increase in DAI, colonic MPO activity and histological lesions (**Figure 7c–e**). To confirm the deleterious effect of aluminum on colitis healing, we designed a subsequent experiment where aluminum was started just after DSS-induced colitis (**Figure 8a**). In contrast to control animals, which completely recovered their initial body weight 10 days after DSS-induced colitis, administration of AluCi significantly delayed weight gain and led to a sustained increase in colonic weight/size ratio compared with control animals (**Figure 8b,c**).

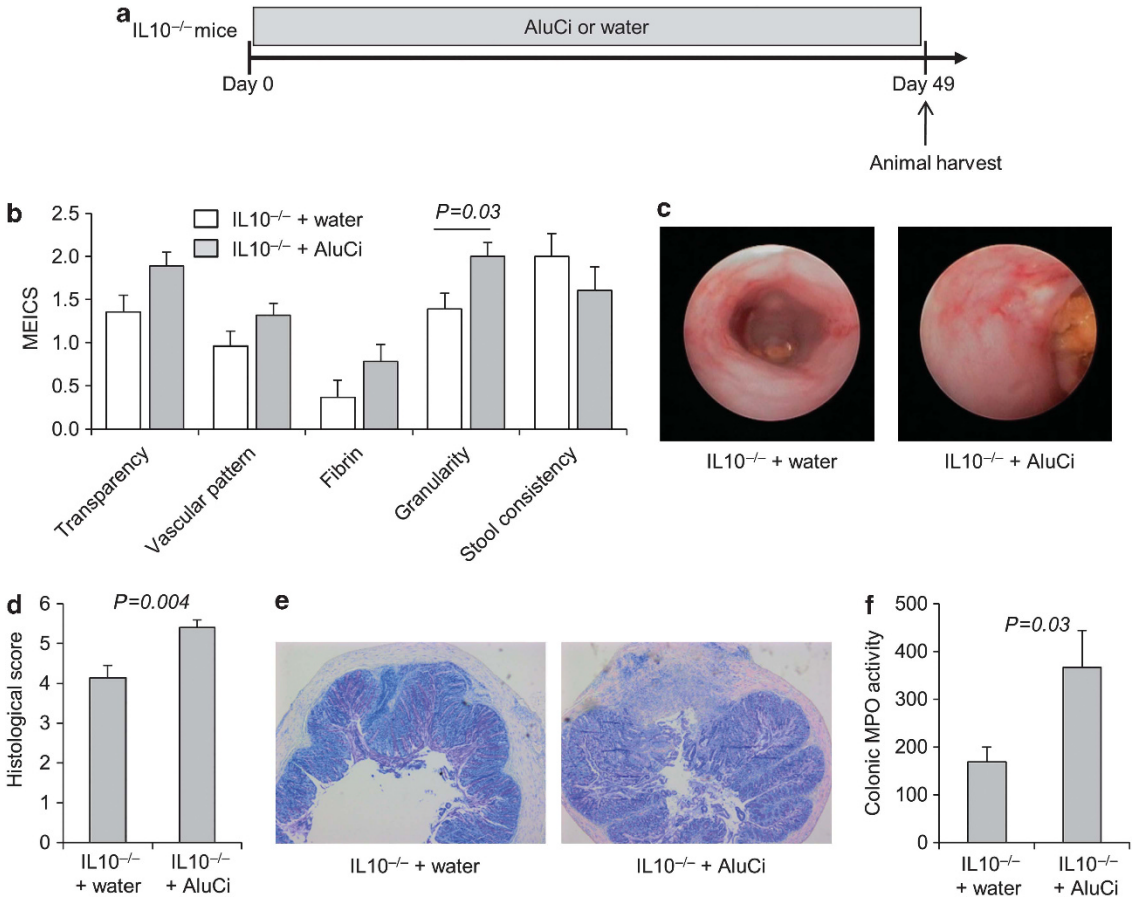

Figure 4 Aluminum citrate (AluCi) aggravates chronic colitis in interleukin 10-negative ($IL10^{-/-}$) mice. (**a**) Eight-week-old $IL10^{-/-}$ mice were treated with AluCi (1.5 mg of Al element kg^{-1} per day) in their drinking water ($n = 15$) or with water only ($n = 14$) for 49 days. (**b**) The five parameters of the murine endoscopic index of colitis severity (MEICS) were determined. (**c**) Mini-endoscopic images were done as described in Methods. (**d**, **e**) Histopathological changes in colon tissues were examined by May-Grünwald and Giemsa (MGG) staining and scoring was performed as described in Methods. (**f**) Myeloperoxidase (MPO) activity was measured in colonic lesions.

To better evaluate the effects of aluminum on colonic wound healing, we quantified *ex vivo* epithelial cell proliferation and apoptosis in the colon of C57BL6 mice receiving or not receiving aluminum 10 days after DSS-induced colitis (**Figure 9a**). AluCi administration was associated with an inhibition of epithelial cell proliferation, as assessed by proliferating cell nuclear antigen (PCNA) immunostaining, compared with control animals (**Figure 9a,b**). The mean fluorescence of terminal transferase dUTP nick end labeling (TUNEL)-stained colon sections was similar in animals with colitis receiving or not receiving aluminum (**Figure 9c,d**).

To confirm the direct influence of aluminum on epithelial cell proliferation, we performed an explanatory experiment in HT-29 cells. We showed that aluminum inhibited epithelial cell proliferation by $>40\%$ without modification of cell death assessed by lactate deshydrogenase release (**Figure 9e,f**).

Aluminum alters the intestinal barrier and induces granuloma formation

We next assessed the intestinal effects of aluminum given once a day ($1.5\ mg\ kg^{-1}$) for 4 weeks on epithelial barrier integrity. The rate of bacterial translocation, reflecting the intestinal barrier, was very low in the mesenteric lymph nodes (MLN) of control C57BL6 mice receiving PBS (**Figure 10a**). In contrast, more than a 100-fold increased colonization of MLN was observed in animals receiving AluP (**Figure 10a**). Tight junctions of epithelial cells involving occludins, claudins, and zonula occludens are critical to maintain intestinal barrier function. A significant decrease in occludin (*Ocln*) mRNA expression was observed in the colon of mice treated with aluminum compared with PBS-treated control animals (**Figure 10b**). We then evaluated the effect of aluminum on colonic flora bulk and composition. Both remained similar in the colon of mice receiving aluminum or PBS (**Figure 10c**). Altogether, these data suggest that aluminum enhanced intestinal permeability leading to an increased load of bacteria through the intestinal wall without a concomitant increase in bacterial pressure in the colon.

The number and size of granulomas developed *in vitro* was evaluated after a 4-day incubation of human peripheral blood mononuclear cells (PBMCs) from healthy donors with increasing concentrations of AluP alone and/or together with *Mycobacterium bovis* strain BCG (BCG), adherent/invasive *Escherichia coli* strain LF82 (AIEC) and a non-pathogenic

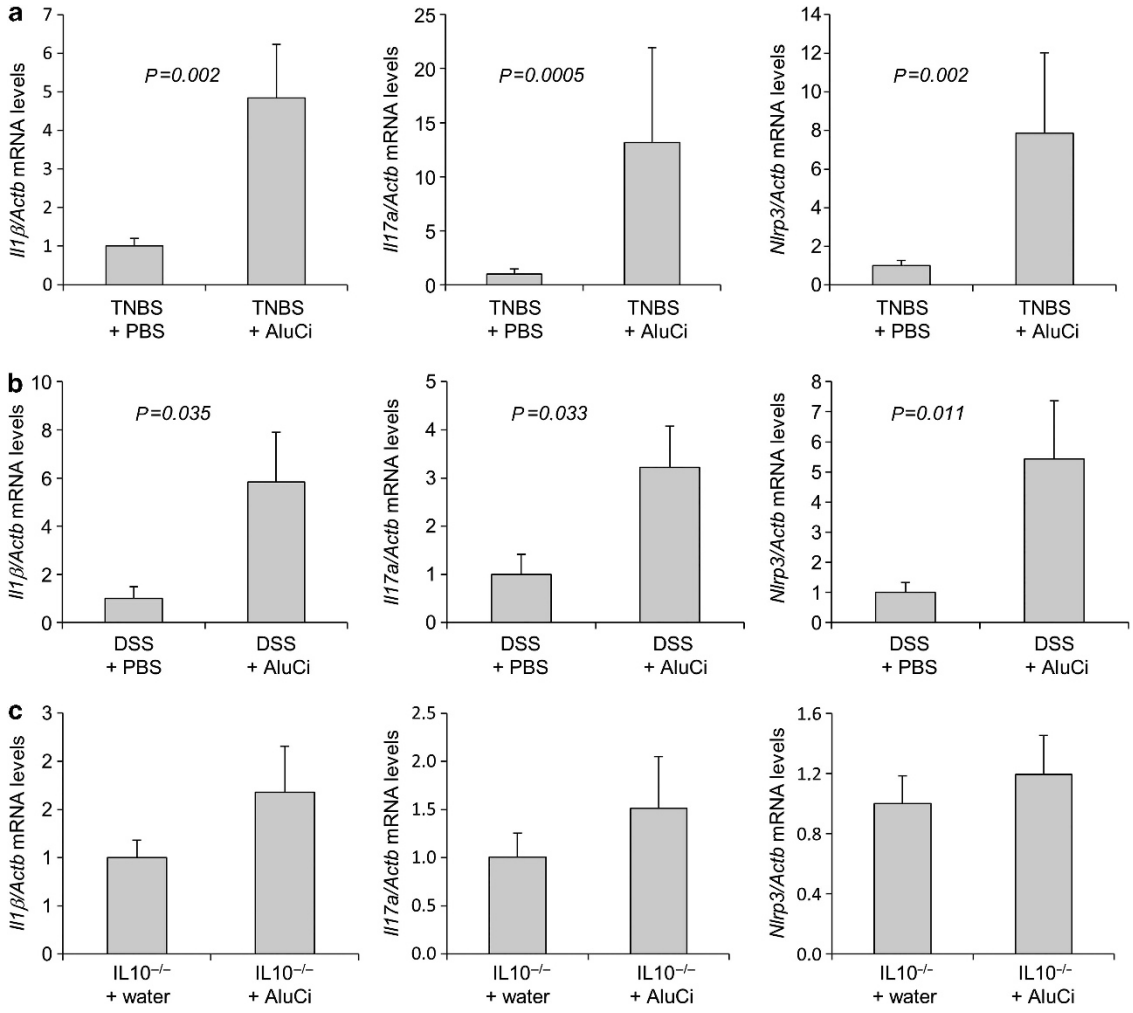

Figure 5 Aluminum citrate (AluCi) increases the expression of pro-inflammatory cytokines in colitis. *Il1*β, *Il17a*, and *Nlrp3* mRNA levels from homogenized colons of (**a**) mice treated with 2,4,6-trinitrobenzene sulfonic acid (TNBS) and phosphate buffer saline (PBS) or treated with TNBS and AluCi, (**b**) mice treated with dextran sodium sulfate (DSS) and PBS or treated with DSS and AluCi, and (**c**) interleukin 10-negative ($IL10^{-/-}$) mice treated or not with AluCi.

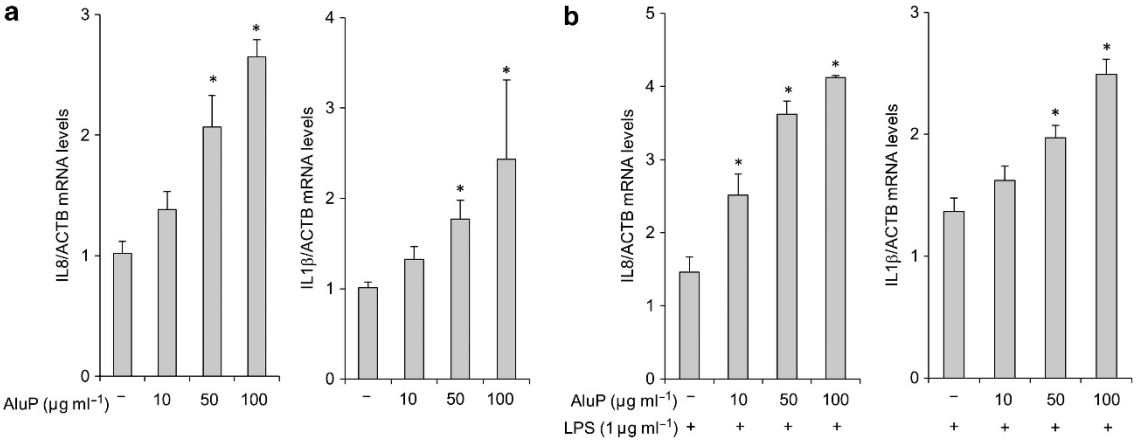

Figure 6 Aluminum phosphate (AluP) stimulates the expression of interleukin 8 (IL8) and IL1β by intestinal epithelial cells and enhances their response to bacterial stimuli. (**a**) Caco-2 cells were incubated with increasing doses of AluP (from 10 to 100 μg of Al element ml^{-1}). qPCR assay on Caco-2 cell lysates showed a dose-dependent increase in IL8 and IL1β expression in the presence of aluminum. (**b**) Caco-2 cells were co-stimulated with increasing doses of AluP (from 10 to 100 $\mu g\,ml^{-1}$) and lipopolysaccharide (LPS). qPCR assay on Caco-2 cell lysates showed a dose-dependent increase in IL8 and IL1β expression in the presence of aluminum compared with LPS stimulation alone. *$P<0.05$ vs. controls.

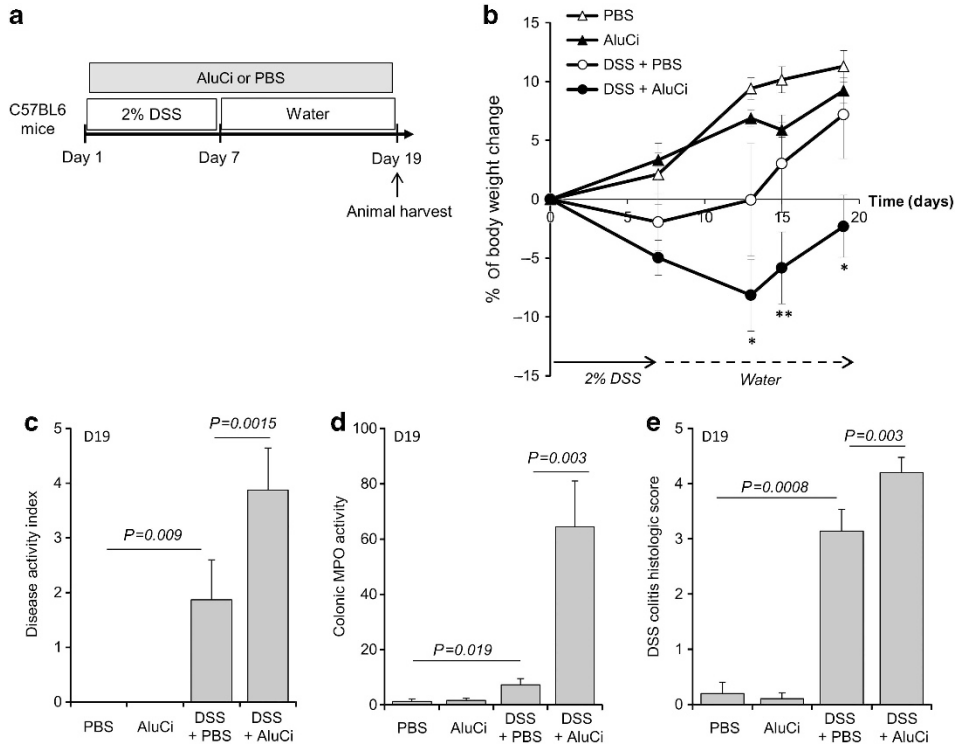

Figure 7 Aluminum citrate (AluCi) extends the duration of dextran sodium sulfate (DSS)-induced colitis. (**a**) C57BL6 mice ($n = 10$–15 per group) were treated with 2% DSS for 7 days, followed by regular drinking water for 12 days. In parallel, mice were treated with AluCi (1.5 mg of Al element kg^{-1} per day) or phosphate buffer saline (PBS) once a day until the end of the experiment. (**b**) Body weight was scored at baseline, D7, D13, D15, and D19. * means $P < 0.05$; ** means $P < 0.01$ between DSS ± PBS and DSS ± AluCi. (**c**) A disease activity index that included body weight variation, the presence of blood in stools, and stool consistency was calculated at day 19. (**d**) Myeloperoxidase (MPO) was measured in colonic samples harvested on day 19. (**e**) Histopathological changes in the colon tissues were examined by May-Grünwald and Giemsa (MGG) staining and scoring of histopathology, as described in Methods.

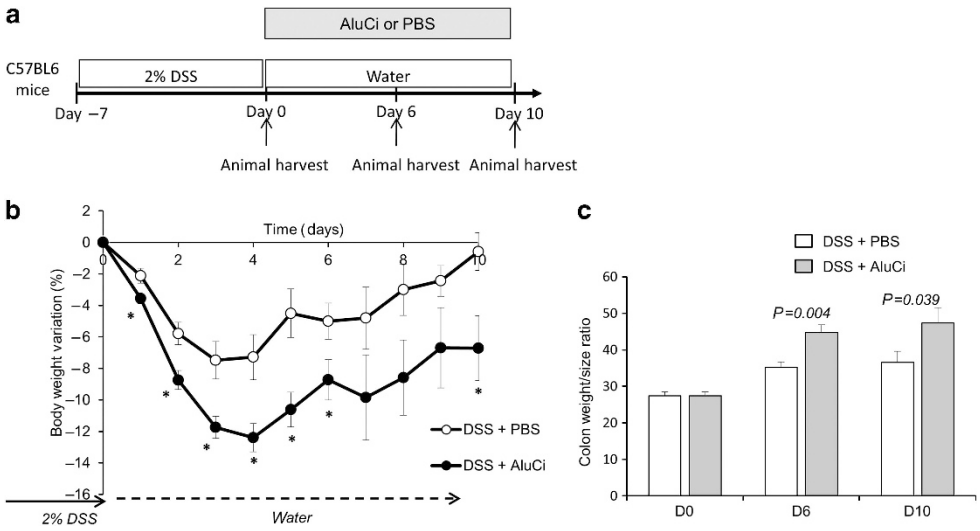

Figure 8 Aluminum citrate (AluCi) decreases the mucosal repair. (**a**) C57BL6 mice were treated with 2% dextran sodium sulfate (DSS) for 7 days, followed by regular drinking water for 10 days. AluCi (1.5 mg of Al element kg^{-1} per day) and phosphate buffer saline (PBS) treatment were started only after DSS discontinuation on day 7. (**b**) Body weight was scored daily. * means $P < 0.05$. (**c**) Colon length and weight were measured from mice euthanized on day 0, day 6, and day 10 after the start of aluminum treatment and the colon weight/size ratio was calculated.

Escherichia coli K-12 strain DH5α.[19,20] As expected, no granulomas were observed in control wells without aluminum and bacteria. The granuloma count increased proportionally until 700 granuloma counts per well with the increased dose of aluminum, with a positive effect beginning at a very low concentration of aluminum (5 ng Al element ml^{-1})

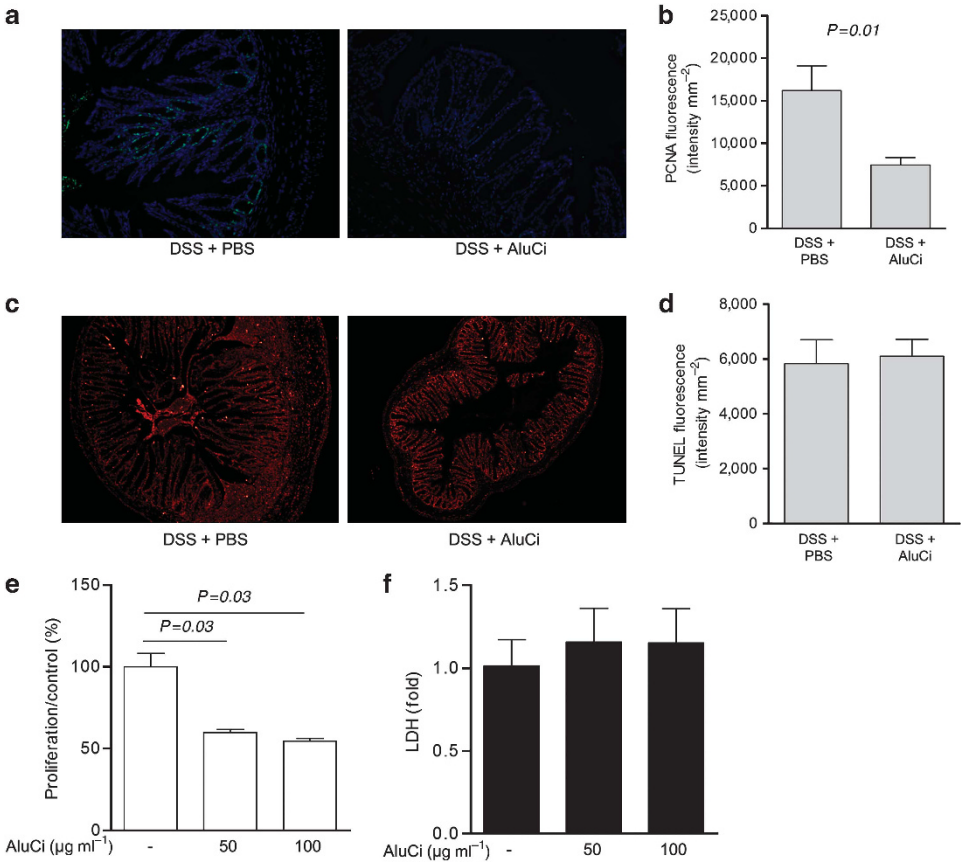

Figure 9 Aluminum citrate (AluCi) inhibits epithelial cell proliferation *in vivo* and *in vitro*. C57BL6 mice were fed with AluCi or phosphate buffer saline (PBS) for 10 days after dextran sodium sulfate (DSS)-induced colitis. (**a**, **b**) Proliferating cell nuclear antigen (PCNA) immunostaining of colon sections (**a**) and its quantification (**b**) showed a decrease in epithelial cell proliferation in mice having received aluminum as compared with mice administered phosphate buffer saline (PBS). (**c**, **d**) Terminal transferase dUTP nick end labeling (TUNEL) immunostaining of the same colons (**c**) and its quantification (**d**) shows no significant difference in epithelial cell apoptosis. Caco-2 cells were incubated with increasing doses of AluCi (50 and 100 $\mu g\,ml^{-1}$) for 5 days. (**e**) MTT assay showed a decrease in epithelial cell proliferation. (**f**) Lactate dehydrogenase (LDH) activity assay in the supernatants did not reveal any significant variation.

(**Figure 10d,e**). Same experiments were performed with Zn and no granuloma formation was observed, showing a specific effect of aluminum (data not shown). We then evaluated the effect of a suboptimal concentration of aluminum (5 ng ml^{-1}) on bacteria-induced granulomas. As previously described, non-pathogenic *E. coli*, AIEC, and mycobacteria induced granulomas formation, with a mean number per well of 101.5 ± 24.5, 224.5 ± 72.3, and 278.8 ± 47.3, respectively.[20] Aluminum at the dosage of 5 ng ml^{-1} potentiated the effect of bacterial infection on granulomas formation, resulting in an increased number and a bigger size of granulomas (**Figure 10f**).

Altogether, these data suggest that aluminum administration leads to a leaky gut, enhancing intestinal bacterial translocation and favoring development of granulomas.

DISCUSSION

Our study provides strong evidence that aluminum modulates intestinal inflammation *in vivo* in mice. A daily intake of aluminum at a concentration observed in the environment increased the severity as well as the duration of intestinal inflammation with impaired mucosal repair in different models of colitis in mice. Aluminum mediated intestinal inflammation through several mechanisms, including inflammatory response against bacteria, epithelial cell renewal and occludin expression, which affected the intestinal barrier and favored granulomas formation.

In humans, the principal route of entry of aluminum is the ingestion of food or water containing aluminum.[12,13] Oral bioavailability of aluminum is estimated to be $<1\%$.[21] Aluminum accumulates in the skeletal system and the brain, and a link with diseases such as osteomalacia and encephalopathy, Alzheimer and Parkinson's diseases have been reported.[16,22,23] The low percentage of oral bioavailability of aluminum is actually misleading. In fact, after oral administration, 40% of the ingested dose accumulates within the intestinal mucosa, which makes the gut the main storage organ for aluminum in the body.[24,25] Intestinal accumulation of aluminum may be particularly relevant to Crohn's disease since it has been identified within macrophages of Peyer's patches but also around dilated submucosal lymphatics and in MLN.[26–28]

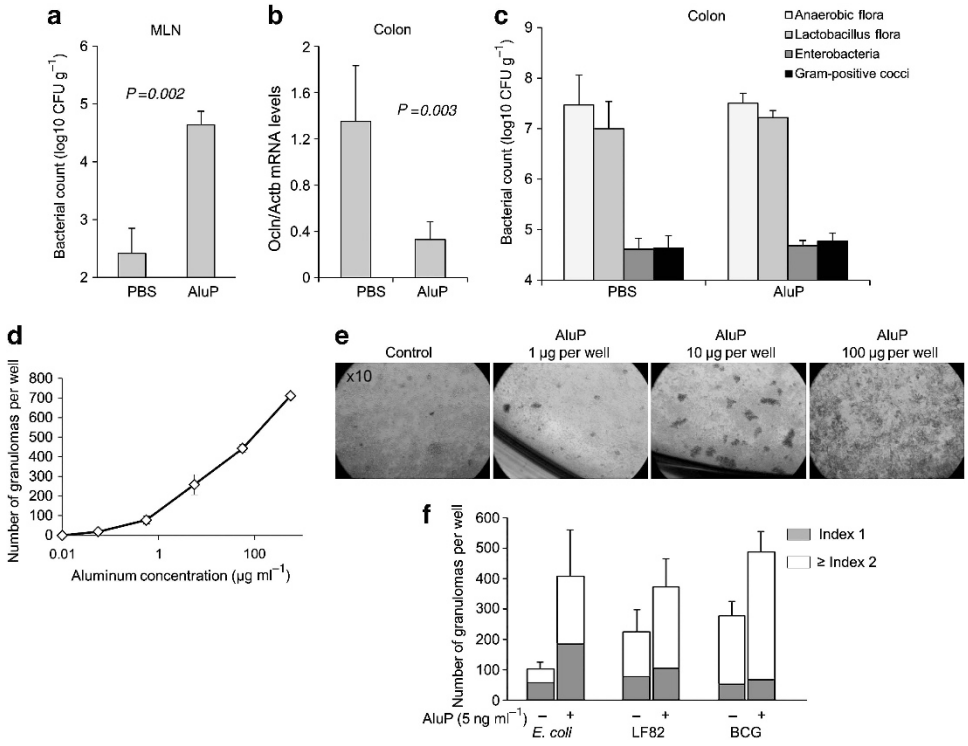

Figure 10 Aluminum alters intestinal barrier integrity and induces granuloma formation. C57BL6 mice were fed with aluminum phosphate (AluP) (1.5 mg of Al element kg^{-1} per day, $n=9$) or phosphate buffer saline (PBS) ($n=4$) for 4 weeks. Bacterial counts in mesenteric lymph nodes (MLN) and colon were determined after 4 weeks. (**a**) Bacterial counts in MLN were significantly higher in aluminum-treated mice than in PBS-treated mice. (**b**) RT-qPCR assay of homogenized colons showed a decrease in *Ocln* mRNA in mice treated with aluminum as compared with PBS-treated mice. (**c**) Bacterial count of specific strains in the colonic mucosa showed no difference between aluminum-treated and PBS-treated mice. (**d**) Human peripheral blood mononuclear cells (PBMCs) were incubated for 4 days with increasing doses of AluP (from 1 to 100 μg of Al element per well; 1.5 ml medium per well). Quantitative analysis of the number of granulomas showed a dose-dependent enhancement of granuloma number in response to aluminum. (**e**) Representative light microscopy pictures ($\times 10$) of the culture wells after 4 days of reaction revealed large multicellular structures (granulomas) in the presence of aluminum. (**f**) Human PBMCs were incubated for 5 days with non-pathogenic *E. coli* K-12 strain DH5α, AIEC strain LF82 or BCG, alone or in the presence of a low dose of aluminum (5 ng of Al element ml^{-1}). The number of granulomas according to their size (Index 1, small size, Index 2, big size) was counted. CFU, colony forming unit.

In spite of this, the potential toxic role of aluminum in the gut has been poorly studied. Interestingly, a fatal outbreak of granulomatous enteritis with many histological similarities with Crohn's disease was reported in a group of horses sharing a common environment. In the evaluation of the cluster, an unexpected finding was the presence of aluminum excess in affected tissues.[29] Our results are in agreement with a study reported only in the abstract form, in which oral aluminum increased histological scores in IL10 knockout mice.[30] Moreover, using two different experimental models of chemically induced colitis developed in mice with different genetic backgrounds, we here demonstrated that small amounts of two different forms of aluminum enhanced the intensity and duration of intestinal inflammation, leading to an increased mortality, increased body weight loss, more intense macroscopic and histological lesions, and enhancement of colonic MPO activities.

Importantly, the dose ($1.5\,mg\,kg^{-1}$) and the route of aluminum administration used in this study are relevant to human exposure. Indeed, it was estimated by a US food additives survey that most Americans ingest from 0.01 to 1.4 mg total aluminum per kg body weight per day. In the same study, it was estimated that $\sim$5% of Americans ingested >95 mg aluminum per day (>1.36 mg per kg body weight) as additives in commercially processed foods and beverages.[16] In Europe, it was also estimated that the tolerable intake of aluminum is exceeded in a significant proportion of the population, especially in children, who are more vulnerable to toxic effects of pollutants than adults.[31,32] Moreover, these estimations did not take into account aluminum ingestion through pharmaceuticals, which is estimated to account for 99% of the aluminum ingested by individuals consuming aluminum-containing medications.[33] Aluminum can be found naturally in different forms, we thus choose to study an organic soluble form (citrate) and a particular form (phosphate). Our results demonstrated that both forms of aluminum worsened colitis and delayed mucosal healing, excluding a form-based effect.

The precise mechanisms involved in the detrimental effects of aluminum on intestinal inflammation are unknown. Aluminum has potential direct cytotoxic effects at high concentrations but most of its biological mechanisms of action

have been described when looking at its adjuvant effect in vaccines.[34] In the latter case, aluminum-induced inflammation involves the Nlrp3 inflammasome but also Nlrp3-independent effects mediated through macrophages, B and T cells, resulting in an enhanced antigen-specific T-cell response and an increased production of inflammatory cytokines.[35] In the present study, no direct intestinal cytotoxic effect of aluminum was detected in control animals fed for 1 month with small amounts of aluminum, nor when epithelial cells were cultured with high concentrations of aluminum reaching 0.1 mg ml^{-1}. Consistent with previous studies analyzing in the skin or the lung the immunobiology of intradermal or inhaled aluminum, oral exposure to aluminum activated Nlrp3 and potentiated the expression of several inflammatory cytokines.[36,37] Furthermore, evidence supporting a key role of epithelial cells in aluminum-sustained intestinal inflammation was obtained both *in vitro* and *in vivo* and was in line with a previous study showing that aluminum decreased the transepithelial electrical resistance of Caco-2 cells.[34] Using two different HT-29 and Caco-2 epithelial cell lines, aluminum, in a dose-dependent manner and synergistically with bacterial LPS, enhanced the production of inflammatory cytokines and decreased by $>40\%$ their ability to proliferate. The relevance of our *in vitro* data was further highlighted by the demonstration that animals treated with aluminum presented an impaired epithelial wound healing, with sustained inflammation and an increased bacterial translocation to MLNs. Another mechanism of action of aluminum may be through its direct interaction with bacterial flora. In our experiments, aluminum did not modify the bacterial composition of the colonic flora of mice. It has been hypothesized that aluminum, through metal chelating systems, could gain access to microorganisms and then alter their pathogenicity and ability to induce an exuberant granulomatous response.[38] We here demonstrated that aluminum was indeed capable of stimulating granulomas formation, either alone or when associated with bacteria.

Translation of experimental evidence to human diseases remains hazardous. Aluminum exposure has already been implicated in a variety of chronic undetermined inflammatory diseases, such as multiple sclerosis, myofasciitis, pulmonary granulomatosis, and rheumatoid arthritis.[39–42] Since most people living in industrialized and emerging countries are routinely and inevitably exposed to aluminum, future descriptive, genetic, and epidemiological studies will be necessary to clarify the mechanisms leading to aluminum susceptibility in patients. An emerging concept suggests that dysfunction of xenobiotic processing enzymes expression or activity in the intestinal mucosa may be an important event in the initiation and progression of IBD.[43,44] Indeed, several studies have identified an association between single-nucleotide polymorphism in genes involved in xenobiotics detoxification and susceptibility to IBD.[45,46] New research activities should now develop standard protocols for measuring aluminum in intestinal tissues of patients with IBD and controls, and analyze these data according to the genetic profile of their detoxification enzymes.

METHODS

Animals. Five- to eight-week-old C57BL6 and BALB/C male mice were purchased from Janvier Laboratory (Le Genest-St-Isle, France). Animals were maintained under specific pathogen-free conditions in the animal facility at the Institut Pasteur de Lille. B6-IL10tm1Cgn ($IL10^{-/-}$) mice were bred in the animal facility of the University Hospital of Zurich. Animals had access to standard tap water and chow diet *ad libitum*. All animal experiments were approved by the local animal care program and were in accordance with the European convention on research animal protection.

Aluminum treatment. Aluminum phosphate ($AlH_6O_{12}P_3$; Sigma-Aldrich, Saint-Quentin Fallavier, France) or aluminum citrate ($AlC_6O_7H_5$) was diluted in PBS (Lifetechnologies, Saint Aubin, France) and administered once a day with a gavage needle at a concentration of 1.5 mg Al element per kg body weight, an amount equivalent to the high end of the total aluminum range ingested daily by humans living in contemporary urban society.[16] The duration of aluminum treatment was dependent on the setting of each experiment and was detailed in each figure. A dose-response experiment was performed and AluP was given to mice at a concentration of 0.15, 1.5, and 15 mg Al element per kg body weight per day. Zinc phosphate ($Zn_3(PO_4)_2$) diluted in PBS was used as a control and was orally administered to mice at a concentration of 1.5 mg Zn element per kg body weight per day. Stock solutions of aluminum salts or ZnP, adjusted to mice weight, were prepared weekly. In all experiments, control mice received PBS by gavage.

For experiments performed with $IL10^{-/-}$ mice, AluCi was diluted in their drinking water at a concentration of 0.015 mg Al element ml^{-1} to reach a daily exposure of 1.5 mg Al element per kg body weight.

Induction of TNBS and DSS colitis. TNBS colitis was induced in anesthetized C57BL6 mice by intrarectal administration of TNBS (150 mg kg^{-1}; Sigma-Aldrich) diluted in a 1:1 (v/v) mix of 0.9% NaCl and 100% ethanol, as described previously.[47] Control animals received an NaCl/ethanol mix using the same technique. Mice were euthanized 4 days after TNBS/ethanol administration.

Acute colitis was induced with 2.5% (w/v) DSS (45 kDa; TdB Consultancy, Uppsala, Sweden) dissolved in water for 7–9 days. For recovery experiments, colitis was induced by feeding mice with 2% (w/v) DSS for 7 days, followed by normal water until the end of the experiments, 10 or 12 days after DSS discontinuation. At the end of each experiment, mice were assessed for clinical score and euthanized.

Determination of clinical scores. For TNBS-induced colitis, animals were euthanized and the colon of each mouse was dissected and cut longitudinally to reveal the colonic mucosa. The intensity of colonic lesions was first evaluated macroscopically according to the Wallace score.[48] The Wallace score rates macroscopic lesions on a scale from 0 to 10 based on features reflecting inflammation, such as hyperemia, thickening of the bowel, and the extent of ulceration. A colon specimen located within the ulceration was used for histological evaluation. The other parts of the colon were frozen for subsequent analysis of mRNA expression and MPO activity quantification.

For DSS-induced colitis, body weight was determined regularly during DSS and the water administration phase until the end of each experiment. At the end of each experiment, animals were assessed for clinical score by recording body weight variation, stool consistency, and occult blood before being euthanized. A DAI was determined as previously described and is summarized in **Supplementary Table 1** online.[49] Rectal bleeding was assessed with the ColoScreen III Lab Pack (Elitech, Salon-de-Provence, France). The DAI score ranged from 0 (healthy) to 12 (greatest level of colitis). After euthanasia, the colon was carefully dissected and its weight and size were measured. Circular sections of the colon were prepared for histological analysis. The other parts of the colon were frozen for subsequent analysis of mRNA expression and MPO activity quantification.

In the model of chronic colitis, IL10$^{-/-}$ animals were anesthetized intraperitoneally with a mixture of 100 mg ketamine (Vétoquinol, Bern, Swizerland) and 8 mg of Xylazine (Bayer, Lyssach, Switzerland) per kg body weight and examined as described previously with the Tele Pack Pal 20043020 (Karl Storz Endoskope, Tuttloingen, Germany).[50] Colonoscopy was scored using the murine endoscopic index of colitis severity scoring system as described previously.[51] After euthanasia, circular sections of the colon were prepared for histological analysis. The other parts of the colon were frozen for subsequent analysis of mRNA expression and MPO activity quantification.

Histology. Colons were fixed in 4% paraformaldehyde, and embedded in paraffin (Labonord, Templemars, France). Tissue sections were stained with May-Grünwald and Giemsa and evaluated blindly by two investigators. Histological lesions of mice with TNBS-induced colitis were quantified using the modification by Ameho of the histopathological grading system of Macpherson and Pfeiffer (ranging from 0 to 6).[48] Briefly, histological findings identical to those of normal mice were scored as 0, mild mucosal and/or submucosal inflammatory infiltrate and edema, punctate mucosal erosions, and intact muscularis mucosae were scored as 1, the same histological findings involving 50% of the specimen were scored as 2, prominent inflammatory infiltrate and edema, deeper areas of ulceration extending through the muscularis mucosae into the submucosa, and rare inflammatory cells invading the muscularis propria but without muscle necrosis were scored as 3, the same histological findings involving 50% of the specimen were scored as 4, extensive ulceration with coagulative necrosis with deep extension of the necrosis into the muscularis propria were scored as 5, and the same histological findings involving 50% of the specimen were scored as 6.

For DSS-induced colitis and chronic colitis, histological lesions were assessed using a score quantifying the intensity of the inflammatory cell infiltrate (scores 0–3) and the tissue damage (scores 0–3) as previously described.[49] Briefly, the presence of occasional inflammatory cells in the lamina propria was scored as 0, increased numbers of inflammatory cells in the lamina propria as 1, confluence of inflammatory cells extending into the submucosa as 2, and transmural extension of the infiltrate as 3. For tissue damage, scores were 0, no mucosal damage; 1, lymphoepithelial lesions; 2, surface mucosal erosion or focal ulceration; 3, extensive mucosal damage and extension into deeper structures of the bowel wall. The combined histological score ranged from 0 (no changes) to 6 (extensive infiltration and tissue damage).

MPO activity measurement. MPO activity was measured to monitor the degree of neutrophil infiltration in the colonic lesions during chemically induced and chronic colitis.[52] Colon specimens were homogenized with an Ultra Turrax T8 (Ika-Werke, Staufen, Germany) in a phosphate buffer (pH 6.0) containing 0.5% hexadecyltrimethyl ammonium and subjected to two sonication and freeze-thaw cycles. The suspensions were centrifuged at 14,000 × *g* for 15 min at 4 °C and the supernatants were reacted with 1 mg ml^{-1} o-dianisidine hydrochloride and 0.0005% hydrogen peroxide. The optical density of each sample was read at 450 nm with a Versamax microplate reader (MDS Analytical Technologies, Saint-Grégoire, France). One unit of MPO activity was defined as the amount that degraded 1 µmol peroxidase per minute at 25 °C. The results were expressed as absorbance per total quantity of proteins determined by the Bradford method.

PCNA staining and TUNEL. *Ex vivo* cell proliferation was assessed by staining for PCNA. Colonic sections were boiled in 0.1 M sodium citrate buffer pH 6.0 for 6 min for antigen unmasking. After washing, sections were blocked for 30 min with 5% bovine serum albumin in PBS, stained overnight at 4 °C with anti-PCNA antibody (1/50) (Santa Cruz Biotechnology, Dallas, TX), and incubated with Alexa 488 conjugated secondary antibody (1/100) (Invitrogen, Saint-Aubin, France) for 1 h. Sections were counterstained with DAPI (Molecular Probes, Eugene, OR). To ensure specificity of immunostaining, control sections underwent simultaneous staining with isotype control antibody.

Detection of apoptosis was performed by TUNEL assay using the *in situ* cell death detection kit (Roche, Meylan, France). Sections were permeabilized with 1% Triton X-100, 0.1% sodium citrate, washed and stained for TUNEL according to the manufacturer's instructions. Sections were counterstained with DAPI.

The quantification of positive TUNEL- or PCNA-stained cells was performed randomly using the ImageJ processing and analysis software (NIH, Bethesda, MD). Images were acquired with a DM5500B microscope equipped with a DFC 310 FX camera (Leica Microsystems, Nanterre, France) and mucosal layers were photographed at a magnification of × 10 to measure specific fluorescence intensity.

Cell line stimulation assay. Caco-2 and HT-29 epithelial cells were cultured in 12-well plates (density of 5×10^5 cells per well) with Dulbecco's modified Eagle's medium supplemented with 10% fetal bovine serum (Eurobio, Courtaboeuf Cedex, France) and 1% penicillin-streptomycin (Invitrogen), at 37 °C in 5% CO_2/95% humidified air. Cells were treated with AluP at different concentrations (10–100 µg Al element ml^{-1}) with or without LPS (1 µg ml^{-1}; Sigma-Aldrich) for 3–6 h. After the incubation period, cells were washed twice with sterile PBS, then lysed with RA1 buffer containing 1% β-mercaptoethanol (Macherey-Nagel, Düren, Germany).

For the determination of cytotoxicity and proliferation, cells were incubated with aluminum for 5 days. Supernatants were collected for lactate deshydrogenase measurement (Cytotoxicity detection kit; Roche) and cell proliferation was assessed using a colorimetric MTT cell proliferation assay (Interchim, Montluçon Cedex, France). Optical density was read at 500 and 570 nm, respectively, with a Versamax microplate reader (MDS Analytical Technologies).

RNA extraction and real-time qPCR. Total RNA was extracted from colonic samples with the NucleoSpin RNAII commercial kit (Macherey-Nagel), as described by the manufacturer. cDNA was prepared with the High Capacity cDNA Archive kit and RT–qPCR was performed with SyBrGreen (Applied Biosystems, Saint-Aubin, France). Beta-actin was used as a reference gene and primer sequences are listed in **Supplementary Table 2**.

Microbiologic analysis. Colon samples and MLN were introduced into pre-weighed vials containing 1.5 ml of cysteinated Ringer's solution. After physical disruption of the colon specimens, 10-fold dilutions were performed in the same diluent (decimal dilutions from 10^{-2} to 10^{-5}). Each dilution was spread onto plates of non-selective blood agar (modified Columbia agar) incubated at 37 °C for 1 week under anaerobic conditions, McConkey plates (BioMerieux, Marcy l'Etoile, France) incubated at 37 °C for 48 h under aerobic conditions, and Man, Rogosa, Sharpe plates incubated at 37 °C for 48 h under CO_2-enriched conditions. Total counts were performed, and different types of colonies were subcultured and identified following established morphological and biochemical criteria. Quantitative results are expressed in log colony forming unit(CFU) g^{-1}. The threshold of detection is 10^4 CFU g^{-1}.

After disruption of MLN in the Ringer's solution, 1 ml was grown in brain-heart enrichment broth and 0.1 ml was spread onto plates of non-selective blood agar and incubated at 37 °C for 1 week under anaerobic conditions. If the brain-heart enrichment broth became turbid, then 0.1 ml was spread onto plate of non-selective blood agar and incubated at 37 °C for 1 week under anaerobic conditions. Subcultured bacteria were identified as above. The threshold of detection was 10^2 CFU g^{-1}. All samples were analyzed in a blind manner.

***In vitro* granulomas formation**. Fresh human blood from healthy volunteers was obtained from the Etablissement Français du Sang and was diluted 1/1 (v/v) with RPMI (Invitrogen), layered gently onto a

ficoll-paque solution (Amersham, Courtaboeuf Cedex, France) and then centrifuged for 40 min at 1,800 r.p.m. PBMCs were collected and washed three times in RPMI medium by 10 min centrifugation at 1,800 r.p.m. Cells were counted with a Malassez cell and diluted to a concentration of 1×10^6 cells ml^{-1} in RPMI media supplemented with 7.5% heat-inactivated human AB serum (Sigma-Aldrich). PBMCs were then incubated in 24-well plates with increasing concentrations of AluP or alone for 4–7 days, at 37 °C in a 5% CO_2 atmosphere. In each well, the number of granulomas was counted. Granulomas enumeration was performed using an inverted microscope and a $\times 4$ objective (Olympus CK40, Olympus, Rungis, France). Pictures were taken using an inverted microscope with a $\times 4$, $\times 10$, or $\times 40$ objective (Nikon TE300 Eclipse, Champigny-sur-Marne, France). For experiments with bacterial stimulation, PBMCs were incubated with 1×10^3 non-pathogenic *E. coli* K-12 strain DH5α, AIEC strain LF82 or 1×10^4 BCG, alone or with AluP (5 ng Al element ml^{-1}) for 4 days at 37 °C in a 5% CO_2 atmosphere. Granulomas enumeration was performed as previously described. Results are represented as the total number of granulomas per well and the percentage of small size (index 1) and big size granulomas (indexes 2–4).

Statistical analysis. Data are presented as the mean ± s.e.m. Comparison between different treatment groups for quantitative variables was performed using the Wilcoxon–Mann–Whitney test. Two-tailed significance tests were used. Kaplan–Meier analysis with log-rank statistics was performed in survival during DSS-induced colitis. A P-value of <0.05 was considered as statistically significant.

SUPPLEMENTARY MATERIAL is linked to the online version of the paper at http://www.nature.com/mi

ACKNOWLEDGMENTS

We thank Sven Gruber for doing IL10$^{-/-}$ mice colonoscopy. This work was supported by grants from the French association François Aupetit, the European Foundation DIGESTSCIENCE and the Institut de Recherche en Environnement Industriel (IRENI) financed by the Communauté Urbaine de Dunkerque, the Région Nord Pas-de-Calais, the Ministère de l'Enseignement Supérieur et de la Recherche (France), the CNRS (France) and the European Regional Development Fund (ERDF).

DISCLOSURE

The authors declared no conflict of interest.

REFERENCES

1. Abraham, C. & Medzhitov, R. Interactions between the host innate immune system and microbes in inflammatory bowel disease. *Gastroenterology* **140**, 1729–1737 (2011).
2. Kabi, A., Nickerson, K.P., Homer, C.R. & McDonald, C. Digesting the genetics of inflammatory bowel disease: insights from studies of autophagy risk genes. *Inflamm Bowel Dis* **18**, 782–792 (2012).
3. Kaser, A., Zeissig, S. & Blumberg, R.S. Genes and environment: how will our concepts on the pathophysiology of IBD develop in the future? *Dig Dis* **28**, 395–405 (2010).
4. Molodecky, N.A. *et al.* Increasing incidence and prevalence of the inflammatory bowel diseases with time, based on systematic review. *Gastroenterology* **142**, 46–54. e42; quiz e30 (2012).
5. Pinsk, V., Lemberg, D.A., Grewal, K., Barker, C.C., Schreiber, R.A. & Jacobson, K. Inflammatory bowel disease in the South Asian pediatric population of British Columbia. *Am J Gastroenterol* **102**, 1077–1083 (2007).
6. Cosnes, J. Tobacco and IBD: relevance in the understanding of disease mechanisms and clinical practice. *Best Pract Res Clin Gastroenterol* **18**, 481–496 (2004).
7. Cosnes, J., Carbonnel, F., Beaugerie, L., Blain, A., Reijasse, D. & Gendre, J.P. Effects of appendicectomy on the course of ulcerative colitis. *Gut* **51**, 803–807 (2002).
8. De Vroey, B., De Cassan, C., Gower-Rousseau, C. & Colombel, J.F. Editorial: Antibiotics earlier, IBD later? *Am J Gastroenterol* **105**, 2693–2696 (2010).
9. Hviid, A., Svanstrom, H. & Frisch, M. Antibiotic use and inflammatory bowel diseases in childhood. *Gut* **60**, 49–54 (2011).
10. Kaplan, G.G. *et al.* The inflammatory bowel diseases and ambient air pollution: a novel association. *Am J Gastroenterol* **105**, 2412–2419 (2010).
11. Ananthakrishnan, A.N., McGinley, E.L., Binion, D.G. & Saeian, K. Ambient air pollution correlates with hospitalizations for inflammatory bowel disease: an ecologic analysis. *Inflamm Bowel Dis* **17**, 1138–1145 (2011).
12. Becaria, A., Campbell, A. & Bondy, S.C. Aluminum as a toxicant. *Toxicol Ind Health* **18**, 309–320 (2002).
13. Nayak, P. Aluminum: impacts and disease. *Environ Res* **89**, 101–115 (2002).
14. Keith, S. Toxicological profile: aluminum. US department of health and human services. Public health service. *Agency for toxic substances and disease registry* (2008) http://wwwatsdrcdcgov/toxprofiles/tpasp?id=191&tid=34.
15. Gourier-Frery, C.F.N. *et al.* Aluminuim: Quels risques pour la santé? Synthèse des études épidémiologiques. Volet épidémiologiques de l'expertise collective InVS-Afssa-Afssaps. Institut de veille sanitaire (2003) http://wwwinvssantefr/publications/2003/aluminium_2003/.
16. Greger, J.L. & Sutherland, J.E. Aluminum exposure and metabolism. *Crit Rev Clin Lab Sci* **34**, 439–474 (1997).
17. Lerner, A. Aluminum is a potential environmental factor for Crohn's disease induction: extended hypothesis. *Ann NY Acad Sci* **1107**, 329–345 (2007).
18. Zaki, M.H., Boyd, K.L., Vogel, P., Kastan, M.B., Lamkanfi, M. & Kanneganti, T.D. The NLRP3 inflammasome protects against loss of epithelial integrity and mortality during experimental colitis. *Immunity* **32**, 379–391 (2010).
19. Puissegur, M.P., Botanch, C., Duteyrat, J.L., Delsol, G., Caratero, C. & Altare, F. An in vitro dual model of mycobacterial granulomas to investigate the molecular interactions between mycobacteria and human host cells. *Cell Microbiol* **6**, 423–433 (2004).
20. Meconi, S. *et al.* Adherent-invasive Escherichia coli isolated from Crohn's disease patients induce granulomas in vitro. *Cell Microbiol* **9**, 1252–1261 (2007).
21. Taylor, G.A., Moore, P.B., Ferrier, I.N., Tyrer, S.P. & Edwardson, J.A. Gastrointestinal absorption of aluminium and citrate in man. *J Inorg Biochem* **69**, 165–169 (1998).
22. Meyer-Baron, M., Schaper, M., Knapp, G. & van Thriel, C. Occupational aluminum exposure: evidence in support of its neurobehavioral impact. *Neurotoxicology* **28**, 1068–1078 (2007).
23. Malluche, H.H. Aluminium and bone disease in chronic renal failure. *Nephrol Dial Transplant* **17** (Suppl 2), 21–24 (2002).
24. Cunat, L., Lanhers, M.C., Joyeux, M. & Burnel, D. Bioavailability and intestinal absorption of aluminum in rats: effects of aluminum compounds and some dietary constituents. *Biol Trace Elem Res* **76**, 31–55 (2000).
25. Powell, J.J., Ainley, C.C., Evans, R. & Thompson, R.P. Intestinal perfusion of dietary levels of aluminium: association with the mucosa. *Gut* **35**, 1053–1057 (1994).
26. Shepherd, N.A., Crocker, P.R., Smith, A.P. & Levison, D.A. Exogenous pigment in Peyer's patches. *Hum Pathol* **18**, 50–54 (1987).
27. Urbanski, S.J., Arsenault, A.L., Green, F.H. & Haber, G. Pigment resembling atmospheric dust in Peyer's patches. *Mod Pathol* **2**, 222–226 (1989).
28. Powell, J.J. *et al.* Characterisation of inorganic microparticles in pigment cells of human gut associated lymphoid tissue. *Gut* **38**, 390–395 (1996).
29. Fogarty, U., Perl, D., Good, P., Ensley, S., Seawright, A. & Noonan, J. A cluster of equine granulomatous enteritis cases: the link with aluminium. *Vet Hum Toxicol* **40**, 297–305 (1998).
30. Lerner, A.E.S. & Perl, D. *et al.* The role of aluminum in bacterial-induced colitis in IL-10 deficient mice (abstract). *Gastroenterology* **130**, 362–363 (2006).
31. Burrell, S.A. & Exley, C. There is (still) too much aluminium in infant formulas. *BMC Pediatr* **10**, 63 (2010).

32. Sly, P.D. & Flack, F. Susceptibility of children to environmental pollutants. *Ann NY Acad Sci* **1140**, 163–183 (2008).
33. Greger, J.L. Dietary and other sources of aluminium intake. *Ciba Found Symp* **169**, 26–35. discussion-49 (1992).
34. Aspenstrom-Fagerlund, B., Sundstrom, B., Tallkvist, J., Ilback, N.G. & Glynn, A.W. Fatty acids increase paracellular absorption of aluminium across Caco-2 cell monolayers. *Chem Biol Interact* **181**, 272–278 (2009).
35. Exley, C., Siesjo, P. & Eriksson, H. The immunobiology of aluminium adjuvants: how do they really work? *Trends Immunol* **31**, 103–109 (2010).
36. Vogelbruch, M., Nuss, B., Korner, M., Kapp, A., Kiehl, P. & Bohm, W. Aluminium-induced granulomas after inaccurate intradermal hyposensitization injections of aluminium-adsorbed depot preparations. *Allergy* **55**, 883–887 (2000).
37. Chen, W.J., Monnat, R.J. Jr., Chen, M. & Mottet, N.K. Aluminum induced pulmonary granulomatosis. *Hum Pathol* **9**, 705–711 (1978).
38. Perl, D.P., Fogarty, U., Harpaz, N. & Sachar, D.B. Bacterial-metal interactions: the potential role of aluminum and other trace elements in the etiology of Crohn's disease. *Inflamm Bowel Dis* **10**, 881–883 (2004).
39. Exley, C. *et al.* Elevated urinary excretion of aluminium and iron in multiple sclerosis. *Mult Scler* **12**, 533–540 (2006).
40. Exley, C., Swarbrick, L., Gherardi, R.K. & Authier, F.J. A role for the body burden of aluminium in vaccine-associated macrophagic myofasciitis and chronic fatigue syndrome. *Med Hypotheses* **72**, 135–139 (2009).
41. Sandstrom, R.E. Aluminum induced pulmonary granulomatosis. *Hum Pathol* **10**, 481 (1979).
42. van der Voet, G.B., Dijkmans, B.A., Frankfort, C. & de Wolff, F.A. Elevation of serum aluminium concentrations in patients with rheumatoid arthritis treated with drugs containing aluminium. *Br J Rheumatol* **28**, 144–146 (1989).
43. Roediger, W.E. & Babidge, W. Human colonocyte detoxification. *Gut* **41**, 731–734 (1997).
44. Kaminsky, L.S. & Zhang, Q.Y. The small intestine as a xenobiotic-metabolizing organ. *Drug Metab Dispos* **31**, 1520–1525 (2003).
45. Brant, S.R. *et al.* MDR1 Ala893 polymorphism is associated with inflammatory bowel disease. *Am J Hum Genet* **73**, 1282–1292 (2003).
46. Langmann, T. *et al.* Loss of detoxification in inflammatory bowel disease: dysregulation of pregnane X receptor target genes. *Gastroenterology* **127**, 26–40 (2004).
47. Wirtz, S., Neufert, C., Weigmann, B. & Neurath, M.F. Chemically induced mouse models of intestinal inflammation. *Nat Protoc* **2**, 541–546 (2007).
48. Ameho, C.K. *et al.* Prophylactic effect of dietary glutamine supplementation on interleukin 8 and tumour necrosis factor alpha production in trinitrobenzene sulphonic acid induced colitis. *Gut* **41**, 487–493 (1997).
49. Yan, Y. *et al.* Temporal and spatial analysis of clinical and molecular parameters in dextran sodium sulfate induced colitis. *PLoS ONE* **4**, e6073 (2009).
50. Obermeier, F., Kojouharoff, G., Hans, W., Scholmerich, J., Gross, V. & Falk, W. Interferon-gamma (IFN-gamma)- and tumour necrosis factor (TNF)-induced nitric oxide as toxic effector molecule in chronic dextran sulphate sodium (DSS)-induced colitis in mice. *Clin Exp Immunol* **116**, 238–245 (1999).
51. Becker, C., Fantini, M.C. & Neurath, M.F. High resolution colonoscopy in live mice. *Nat Protoc* **1**, 2900–2904 (2006).
52. Anton, P.M. *et al.* Corticotropin-releasing hormone (CRH) requirement in Clostridium difficile toxin A-mediated intestinal inflammation. *Proc Natl Acad Sci USA* **101**, 8503–8508 (2004).